Studies of the morphology of one-way drawn poly(ethylene terephthalate) films by X-ray diffraction

M. Casey
ICI Ltd Plastics Division, PO Box 6, Bessemer Road, Welwyn Garden City, Hertfordshire, UK
(Received 29 November 1976; revised 29 July 1977)

Films made by stretching amorphous poly(ethylene terephthalate) (PET) in one direction have been examined using techniques of wide- and narrow-angle X-ray diffraction. The films were not subsequently annealed. The in-plane *c*-axis orientation of crystallites was assessed from measurements of reflections from $\bar{1}05$ crystal planes as in the method of Dumbleton and Bowles. However, we found that rather than tending to align parallel to the draw direction, the crystallites tended to lie in two groups inclined at a small angle to the draw direction. The angle of tilt of this 'preferred' direction to the draw axis became smaller for more highly drawn films, and a plot of tensile strength against tilt angle shows a trend to a 'strength limit' for zero tilt. (This tilt must not be confused with the well-known and quite different cyrstalline tilt which occurs after drawn PET is annealed.) Wide-angle diffraction has also been used to estimate crystal dimensions, and low-angle diffraction was used to determine long-period spacings. An analysis of the shape of the diffraction maxima gave an estimate of the shape of the diffracting units, and their influence on mechanical properties is discussed.

INTRODUCTION

In order to achieve enhanced mechanical properties, poly(ethylene terephthalate) (PET) is commonly processed in such a way that molecular orientation is produced in preferred directions. The usual route is to stretch the amorphous polymer at a temperature just above its glass transition. The stretched material may then be annealed under restraint to prevent subsequent heat shrinkage. In the continuous manufacture of biaxially oriented film, for example, a sheet of amorphous PET is obtained by quenching rapidly from the melt. The sheet is stretched in the 'machine-direction', then in the perpendicular 'transverse direction'. This is followed by annealing under restraint and the finished film is reeled-up. There is an extensive literature on the structure of this final annealed state particularly in the case of films and fibres. However, there has been relatively little work on the intermediate state, that is the non-annealed stretched state.

Previous X-ray studies have shown that amorphous PET becomes crystalline when drawn[1] but the wide-angle patterns are often diffuse and dim, particularly at low draw-ratios, making analysis difficult. Dulmage and Geddes[2] showed that the stretching produced alignment of the chain molecules, the chains tending to become parallel to the stretch direction as the draw-ratio increased.

After heat treatment, they found pronounced tilting of the *c*-axes in the crystalline regions, the extent of which depended on the initial draw ratio. This 'annealing tilt' has been observed by others including Heffelfinger and Burton[3], Daubeny, Bunn and Brown[4], and Asano and Seto[5]. In this last work it is clearly established that the extent and direction of the tilt depends on many factors including the initial draw-ratio, the annealing temperature and the type of restraint employed. In the present work measurements have shown the existence of a crystalline tilt in the oriented polymer before annealing, but a rather smaller tilt and in a different direction.

Heffelfinger and Schmidt[6] have estimated crystallite sizes from narrow- and wide-angle X-ray diffraction data, in stretched and heat-set PET, as a function of draw ratio. Statton and Goddard[7] have employed these techniques on heat-set fibre. In the present work similar techniques are used to make such estimates on the unannealed films, but the effects of crystallite imperfections are discussed, effects which are neglected by the above authors.

Low-angle diffraction from the 'strain induced' crystalline state is very dim, so much that it has at times been taken not to exist. The exposures required to obtain photographs in the present samples were often up to a week long. Thus there is little work reported in the literature. Bonart[8] shows a four-point low-angle pattern from stretched, unannealed PET, and Yeh and Geil[9] obtained similar patterns, but only when the polymer was stretched at temperatures so low that considerable voiding occurred. However, the annealed state has been studied in detail by several workers. In fibres, or in tapes which have been drawn without sideways restraint, a four-point pattern is seen which becomes more distinct at higher draw ratios. In one-way drawn films where sideways restraint during drawing produces planar orientation (e.g. drawing over rolls), a four-point pattern is seen when the X-ray beam strikes the film parallel to its surface and a two-point pattern is found when the beam strikes the surface normally[10].

Several models have been proposed to explain the patterns[11] but most of them have been concerned with annealed specimens. The work presented here is interpreted in terms of a fibrillar model, and both narrow- and wide-angle measure-

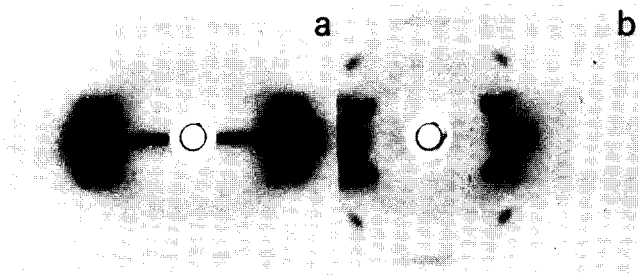

Figure 1 Wide-angle diffraction patterns from one-way drawn PET films, with the X-ray beam incident: (a) normal to; (b) parallel to the film surface

ments are discussed in terms of this model and of the Hosemann theory of paracrystals.

EXPERIMENTAL

The films to be described were made on a pilot plant by ICI Plastics Division. The film is made by stretching amorphous cast sheet over wide rolls. The film passes firstly over a preheating roll which raises the film temperature to about its glass transition (in this series of experiments a preheat temperature of 65°C was used, and the first roll speed was fixed at 0.1 m/sec), then over a draw roll rotating faster than the first. The ratio of the surface speeds of the two rolls defines the 'draw-ratio'. In this way the film is drawn in one direction and restrained by friction in the perpendicular direction. The films were not annealed. The drawing induces crystallization, and as the draw ratio increases, the crystalline volume fraction increases and the crystals become more preferentially oriented, their *c*-axes tending to become parallel to the draw direction and the (100) crystal planes tending to become parallel to the film surface.

This type of orientation results in wide-angle X-ray diffraction patterns as shown in *Figure 1*. The reflections from (100) planes can be seen (large spots) in *Figure 1a* when the incident beam is parallel to the film surface, but not at all in *Figure 1b* when the beam strikes the film surface normally.

Wide-angle X-ray measurements

From wide-angle photographs it was clear that the crystals tended to lie (approximately) with their (100) planes in the plane of the film surface, and with their *c*-axes in the stretching direction. The orientation of the (100) planes was confirmed by goniometric measurements; in reciprocal space the (100) maximum occurred in a position along the direction of the film normal. If the maximum were not exactly along this direction then, by symmetry considerations, two maxima would be observed, corresponding to crystals aligned parallel to and antiparallel to the draw direction. No such doubling was observed. However, the measured (100) peak widths are large (see *Table 1*), so a doubling would only have been seen if it were greater than a few degrees. With this qualification, the results confirm the tendency of the crystals to assume the 'planar' orientation described. We assumed at first that the crystalline *c*-axes would tend to become aligned exactly parallel to the draw direction, but we see later that this was found not to be true.

In our films, the orientation was to be described by three measurements, which specified the angular spread of crystallite orientation measured by rotations around three mutually perpendicular directions marked in *Figure 2* as 1, 2, 3. A 'perfectly' oriented crystal (see below) would lie with its molecular axis in direction 1 and with its (100) plane normals in direction 3, marked a^* in *Figure 2*. As the film is rotated around any one of these three axes, deviations from such 'perfect' orientation may be measured by observing reflections from planes whose normals are perpendicular to the axis. As the specimen is rotated, an intensity maximum is found, and the width of this maximum at half-intensity, ϕ, is used to specify the degree of orientation.

For rotations around axes 1 and 2, measurements were made using reflections from (100) planes, the normals to which lie at 90° to each of these directions. Thus ϕ_1 relates to the 'planar orientation' of crystallites and ϕ_2 to the number of crystal *c*-axis pointing into or out of the film plane.

Measurements were made using a Philips X-ray diffractometer. In practice ϕ_1 for example would be measured by setting the diffractometer to receive reflections from the surface at the (100) Bragg angle 2θ, the specimen being oriented in such a way that the X-rays incident on it travelled in the plane perpendicular to direction 1. By rotating about axis 1 and adjusting the diffraction angle 2θ, the maximum intensity is obtained. The diffraction angle is then fixed and the specimen made to rotate around axis 1. In order to avoid having to make corrections for the change in geometry of the specimen as it rotated, a number of small strips of film were laminated[12] to obtain an approximately rod-shaped bundle whose axis was parallel to direction 1. This was also necessary for measurement of ϕ_2 but not for ϕ_3 since rotation about axis 3 produces no geometry change.

The third measurement, ϕ_3, was to be a measure of the distribution of crystallite *c*-axes in the plane of the film. However, the unit cell of PET is triclinic and there is no strongly reflecting plane whose normal is parallel to the *c*-axis. The nearest is $\bar{1}05$ whose normal lies about 10° from this axis.

In such planar oriented film, the projection of the $\bar{1}05$ normal in the plane of the film is expected to lie 8.5° from the *c*-axis, according to the unit cell of Daubeny, Bunn and Brown[4]. Thus on rotating the sample around axis 3, we find

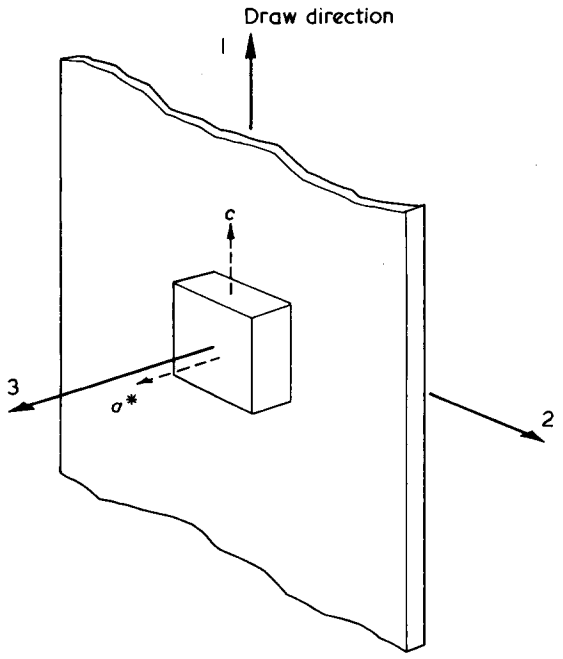

Figure 2 Illustration of the scheme of orientation measurements

two maxima corresponding to reflections from $\bar{1}05$ planes in crystals whose c-axes are pointing parallel and antiparallel to the draw direction. The two maxima overlap considerably, particularly for less well-oriented film, and measurement of their half-width is difficult. In the method of Dumbleton and Bowles[13], the maxima are separated using a numerical method which requires a knowledge of their separation (2α). In view of an uncertainty in the value of α, we determined to measure this separation, and the curves were fitted by computer as illustrated in *Figure 3*. The large peaks are $\bar{1}05$ reflections and the smaller satellite peaks are due to $0\bar{2}4$ reflections. The computer generated two equal pairs of peaks, symmetrically spaced, whose height, width, and distance from the centre of the pattern could be varied, as could the height of a superimposed flat baseline. The sum of these was then compared with the measured scattering intensity and the adjustable parameters chosen to obtain a least squares fit. The peak shape was taken to be a Gaussian, but in practice the method was relatively insensitive to shape, the separation being almost identical when using a Lorentzian form. The value of α was then taken as the angular separation between the centre of the pattern and the computer-generated $\bar{1}05$ peak. From this procedure we have a measure of α and of ϕ_3. *Table 1* gives the values of ϕ and of the tensile breaking strength of the films measured parallel to the draw direction, and we see the expected increase in orientation for the higher draw-ratio, stronger, films.

A more interesting result appears, however, if we plot α against film strength as in *Figure 4*. The angle clearly increases as the draw increases (thus, incidentally, making unsuitable the resolution method suggested by Dumbleton and Bowles) and is usually less than 8.5°. This shift has recently been observed by Bhatt, Bell and Knox[14]. They interpret it in terms of a change in the unit cell parameters. However, the effects of such a change would be seen in other reflections; up to 4% changes in d-spacings are predicted, and although we have observed some small changes in d-spacings with draw-ratio, none is as large as this, or consistent with the cell change proposed by them.

We interpret this shift as being caused by c-axes, rather than tending to align exactly parallel to the draw direction, tending to cluster in two groups slightly inclined to the direction of draw. This is consistent with movements in the positions of other diffraction spots. A plot similar to *Figure 4* may be obtained by using data from the $0\bar{2}4$ peak, although with reduced precision. In particular it is possible to see a splitting of the (010) reflection in the less highly drawn films, in *Figure 5a*, but not in the more highly drawn (*Figure 5b*), an effect which could not be predicted by any change in unit cell parameters.

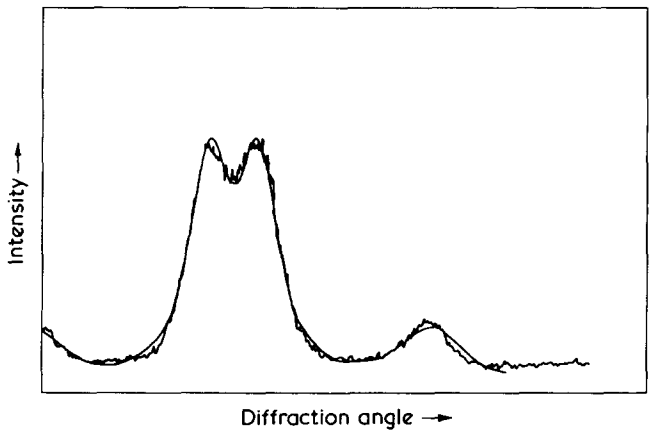

Figure 3 Computer fit to a typical $\bar{1}05$ azimuthal (ϕ_3) scan

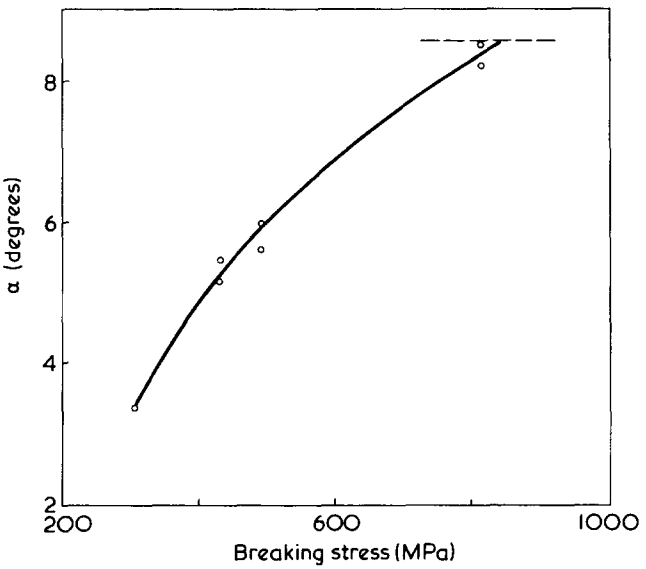

Figure 4 Relationship of measured breaking strength to α

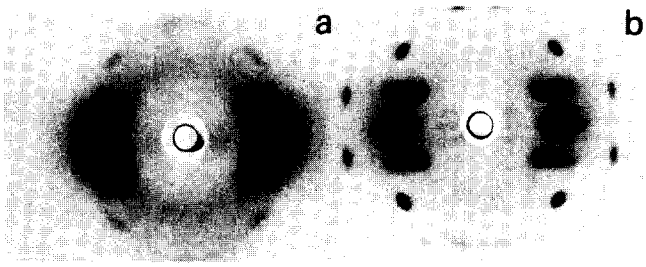

Figure 5 Wide-angle diffraction patterns showing (010) reflection splitting (a) for the lower drawn films, but not for the highest drawn film (b)

Table 1

Draw ratio	Breaking stres (MPa)	Density (kg/m^3)	ϕ_1 (degrees)	ϕ_2 (degrees)	ϕ_3 (degrees)	Long period (nm) (±0.7 nm)	Pattern angle (θ in *Figure 8*) (±1°) (degrees)
3.50:1	218	1365.0	47.1	17.6	7.4	15.2	67
4.00:1	304	1367.7	43.2	17.2	6.3	15.0	66
4.50:1	380	1370.2	40.2	15.6	6.0	15.1	65
5.00:1	437	1374.5	37.3	15.2	5.2	14.8	65
5.25:1	490	1376.0	34.6	13.4	5.1	15.0	65
6.50:1	820	1391.0	20.4	8.6	1.9	15.4	58

In *Table 1* we see the increase in film strength as draw-ratio increased. The effect of drawing more than 6.5:1 was to cause the film to snap, so that a 'strength limit' was encountered. If we return to *Figure 4*, recalling that an increase in α implies a decrease in the angle of tilt of the preferred direction of the *c*-axes to the draw direction, then we can see that for zero tilt, corresponding to $\alpha_0 = 8.5°$ in the Daubeny and Bunn cell, the corresponding film strength is about 840 MPa, which is very close to the strength limit which was actually encountered. (A more recent determination of the unit cell parameters of PET by Fakirov, Fischer and Schmidt[15] puts the value of α_0 as 9.5° rather than 8.5°. This corresponds to a strength of nearly 1000 MPa in *Figure 4*, perhaps implying that some changes in drawing conditions might increase the 'strength limit' somewhat.)

This tilt should not be confused with the well-known and quite different crystalline tilt which occurs after annealing of oriented PET, which was discussed in the Introduction. This has been studied extensively after having been measured first by Daubeny, Bunn and Brown[4]. Annealing produces very large morphological changes in the film, including an increase in density, in long-period spacing[16] and in crystallite orientation. The changes in orientation depend on conditions of annealing as well as on the initial state of the drawn polymer. For example the direction and the extent of the tilt depend on the annealing temperature and amount of mechanical restraint[5]. The present measurements indicate, for the first time, that a preferential *c*-axis tilt occurs in unannealed drawn PET.

In order to obtain the precise direction of the *c*-axis we need to know the unit cell parameters. The unit cell is presently rather in dispute, and unfortunately the resolution of diffraction maxima is not adequate in unannealed samples to define the cell parameters with sufficient precision, because of the broadness of diffraction spots; all published values of the cell parameters have been obtained with annealed samples to produce larger, more perfect crystals[15]. However, we can make measurements of the precise direction of the $\bar{1}05$ normals; the *c*-axis tilt which is measured from α is of course a projection onto the $\vec{3}$ plane. From measurements on wide-angle photographs, the projections onto the $\vec{2}$ plane of $\bar{1}03$ reflections were also measured. This reflection was particularly suitable because both Bunn and Fischer cells predict the same projected angles to the *c*-axis, of about 18.2°. This was close to the measured value of 18° (±0.2°) which did not change with draw-ratio. Thus we conclude that there was no preferred out-of-plane tilt of the *c*-axes.

Crystallite size measurement

An interesting correlation was found when density was plotted against breaking strength in the draw direction. A good straight line was obtained, and this led us to an interest in crystallite size measurements, and their distribution. It is possible to estimate the size of a diffracting crystal from the 2θ broadening of a diffraction spot. The spot is broadened by the limited size of the crystals and by their imperfections. If the crystals could be regarded as perfect, the Scherrer equation[17] gives us this relationship:

$$L_{(hkl)} = \frac{\lambda}{\beta \cos\theta} = \frac{1}{\delta s}$$

where β is the halfwidth and L is the maximum crystallite dimension normal to the reflecting planes. According to Hosemann[17], for crystallite distortions of the type found in polymer crystals, we may split the broadening into two parts:

$$(\delta s)^2 = (\delta s_c)^2 + (\delta s_{II})^2 = \frac{1}{L^2} + \frac{(\pi g_{II})^4 m^4}{d_{hkl}^2}$$

The first term, coming from the Scherrer equation, is due to the limited crystal size, and the second term is the broadening caused by crystalline imperfection. This latter broadening is related to the *d*-spacing of the (*hkl*) planes, the 'order' of the reflection m and to a parameter g_{II}, relating to the deviation of a lattice dimension from perfection.

We have measured the broadening for $\bar{1}05$, 100, 010 and $\bar{1}10$ reflections to obtain an estimate of the above 3-dimensional shape of the crystals, but we see that a value of $m = 5$ for $\bar{1}05$ might introduce serious broadening from imperfections. To examine this, the broadening of $\bar{1}03$ reflections, where we take $m = 3$, was also measured. This plane lies about 20° from the *c*-axis, but it is near enough for these rough measurements. Then plotting δs^2 against m^4 should give a straight line and the crystallite length and g_{II} may be obtained from the intercept and slope, respectively. In *Figure 6* we have drawn a straight line through the two points for each film, and we find that the crystallite *c*-axis length increases gradually as the films are drawn further, (from about 5.7 to ~8.5 nm). The value of g_{II} is always small, less than 1%, probably due to the covalent bonding in this direction.

In the plane perpendicular to the *c*-axis, the broadening of (100), (010), and ($\bar{1}10$) reflections give an idea of the 'weighted average' crystal shape. The bold lines in *Figure 7*

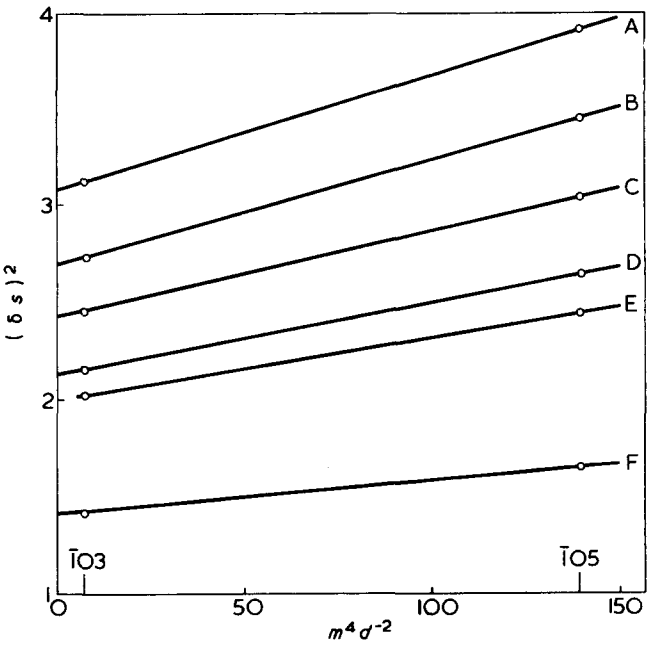

Figure 6 Estimate of the crystallite *c*-length and imperfection assuming Hosemann-type imperfections:

Curve	L (nm)	g_{II} (%)
A	5.7	0.9
B	6.1	0.9
C	6.4	0.8
D	6.9	0.8
E	7.1	0.7
F	8.5	0.6

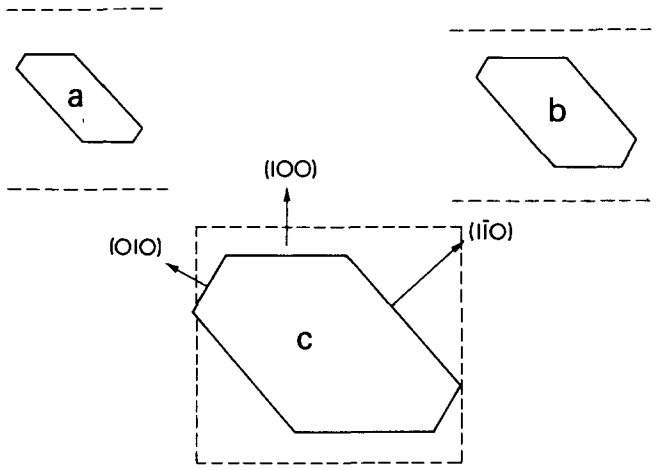

Figure 7 Comparison of estimates of (loaded mean) crystal size perpendicular to the c-axis from the wide angle measurements (——) and small-angle X-ray diffraction (— — —) for the lowest drawn film (a), the highest drawn (c), and an intermediate specimen (b)

show to scale the relative sizes obtained, which changed from about 3 nm in the (100) direction for the lowest drawn sample, marked a in the diagram to 6 nm for the highest-drawn sample marked c. It must be stressed here that these determinations assume the crystallites are perfect, which we know is not true. This causes an underestimate of their size. Thus they give only a rough guide. We shall return to these measurements later to compare with low-angle diffraction measurements (broken lines).

Low-angle diffraction

Photographs were taken using a Franks double-focusing low angle camera with a specimen-to-film distance of 51 mm. Very long exposure times (several days) were required even though the specimens were about 0.5 mm thick (for the perpendicular photographs this thickness was obtained by laminating several layers).

Figure 8a shows schematically the now familiar four-point pattern which is obtained from drawn PET fibres, which in this work was obtained when the beam was incident on the film edge, parallel to its surface. In *Figure 8b* is shown the two-point pattern obtained when the beam strikes the film normally to its surface. Some essential details of the patterns are given in *Table 1*.

In these Figures the diffraction streaks are drawn with their long axes parallel to the equator. In fact at the lowest draw-ratio they could be seen to be inclined slightly to the equator, in the case of the four-point pattern, in such a way as to form a pattern slightly closer to a circle. Because of the diffuseness of this pattern, a measurement of this tilt was not attempted. The higher drawn films showed very little tilt; in the case of the 5:1 draw-ratio film a two dimensional intensity 'map' was constructed which showed an inclination of about 3°, but the accuracy of this measurement must be very low. In the interpretation of the patterns we will assume that the streaks are exactly parallel to the equator.

In the case of parallel photographs, care was taken to avoid the immediate surface region of the film, which might be expected, from previous experience, to be slightly different from the bulk. The perpendicular photographs, taken with the beam traversing the full thickness, would be dominated by the bulk of the film.

Figure 8 also indicates the interpretation we have used for the patterns. Symmetrical spacing of diffraction maxima around the centre of the pattern is due to regularity in the direction of a line joining the maxima. Thus we have regular structures in the directions S, and these are shown as a set of parallel lines. If the maxima were sharp, then the period of this regularity would be inversely related to the angular distance between the maxima, from Bragg's law. Because the maxima are very broad, Bragg's law does not strictly apply, but it is frequently employed to calculate a 'long-period spacing' from the angular separation of the centres of the maxima. This is given in *Table 1*, as is customary, projected onto the direction L. Its value is almost constant at about 15 nm.

The diffraction 'spots' are very broad in the direction ϵ, perpendicular to the draw direction. This type of pattern has been interpreted as being due to the presence of narrow but long microfibrils, consisting of alternating regions of high and low electron density (being crystalline and non-crystalline regions) whose long axes are parallel to the direction of drawing. The model has been discussed by Bonart and Hosemann[18], Statton and Goddard[7], Peterlin[19], Takayanagi[20] and others.

If the regularity were perfect, then an isolated fibril would produce diffraction maxima in which the intensity distribution would be related to the Fourier transform of the diffracting object. Thus a long vertical thin diffracting object would produce a horizontal wide diffraction maximum (a cross-section through a disc in reciprocal space), rather similar to the shape which is observed. However, the fibril will not be isolated and the long-period regularity is very unlikely to be perfect. Pursuing our model, we would expect the spots to be broadened in the directions S by irregularities in the 'long period' spacing and in direction L by the finite fibril length; in direction ϵ the intensity profile will be affected by interference from adjacent fibrils. A (000) reflection is also expected, (or 'central streak'), due to diffraction by the fibril as a unit, and whose intensity is related to the difference in average electron density between the fibril and its surroundings. This zero-order reflection was not observed in any of these samples, indicating that it is very weak. Indeed it is difficult, though possible, to observe one in annealed samples of drawn PET where the intensity of the low-angle pattern is much greater.

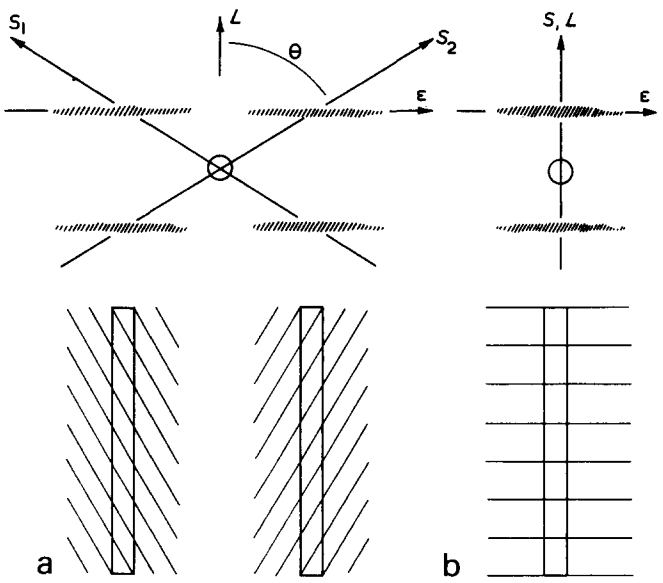

Figure 8 Low-angle X-ray patterns obtained with one-way drawn PET films, and the interpretation used in this work

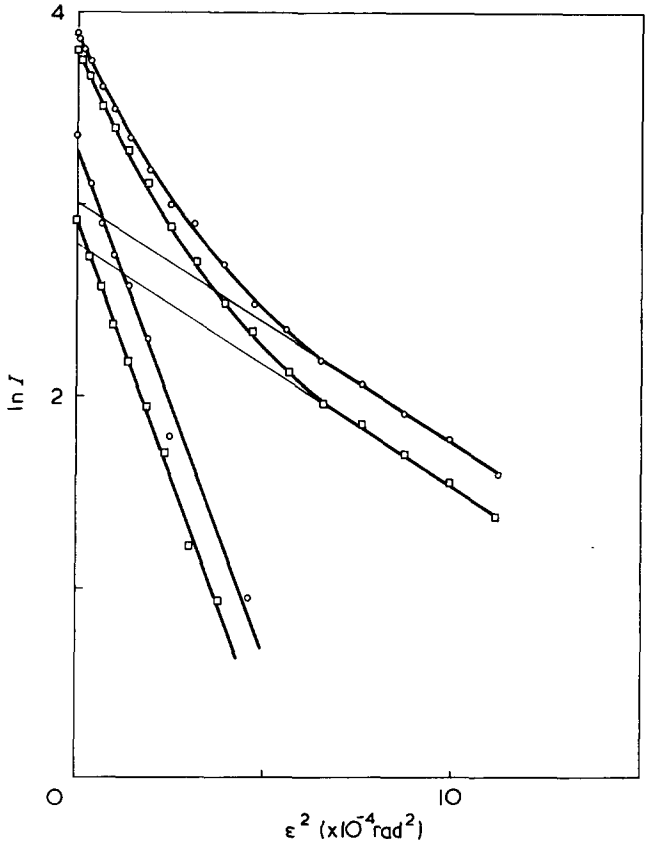

Figure 9 Typical Hosemann-Guinier plots for lowest drawn film

Even when it is observed, the interpretation of the (000) reflection is made difficult because of the possibility of contributions to it from spurious causes such as internal voids or impurities (see for example Heffelfinger and Lippert[10] and Fischer and Fakirov[21]).

Approach of Hosemann

Hosemann has attempted (with other polymers) to quantify the effects described above, by applying his 'paracrystalline lattice' model, described for example in ref 22. In this model the drawn polymer is described as a two-phase structure, of crystals (which make up the fibrils) in a non-crystalline matrix. The crystals find themselves in a large imperfect array which is described as the macroparacrystal, which is defined by six cell parameters and by a set of relative statistical functions which describe the perfection of the macrolattice as measured in different directions.

These parameters are chosen so that the Fourier transform of the macroparacrystal matches the small-angle diffraction pattern. If $f(b)$ is the small-angle scattering amplitude of a single crystallite, which is the 'brick' of the superstructure, then the scattered intensity is proportional to $I(b)$ where:

$$I(b) = \overline{f^2} + \overline{f}^2 (Z - 1)$$

where $Z(b)$ is the paracrystalline lattice factor[22]. The first term is the intensity which would be observed from an isolated crystallite and the second is due to interference from others.

Although the statistics used in the model may take any form, Hosemann uses Gaussian forms for both of the above terms. Thus they are at times separable from diffraction intensity data. Hosemann has analysed many polymers which exhibit two-point diffraction patterns, and in each case the second term above is large in the direction where the regularity is good (the long-period direction), and is much smaller in the perpendicular direction, since the sideways correlation is relatively poor.

It is possible to apply some of these methods to the present measurements, particularly if we bear in mind the physical picture of microfibrils at the same time. For example, if we plot $\ln I$ against ϵ^2 for the intensity profile of a diffraction 'spot', as measured parallel to the equator, then according to Hosemann the slope at high angles relates to $\overline{f}^2$ and thus to the width of the crystalline block, which is the same as the width of the fibril of which it forms a part.

Figure 9 shows such plots from the four points of a pattern obtained from the lowest drawn film, and they have been decomposed in the way Hosemann and Bonart did for polyethylene[18], by firstly drawing a tangent at high angles, then subtracting the extrapolated intensity from the total and replotting the log of the difference. The width of the diffracting unit (fibril) obtained from the gradient at high angles, is 3 nm. The interference term, obtained from the 'difference' gradient, corresponds physically to adjacent fibrils being occasionally 'in register'. Another way of viewing this is that occasionally two adjacent fibrils look like one fibril of double the width. The width which is obtained from the 'difference' gradients is consistently 6 nm, or double the width of the individual unit. It is interesting that these two sizes, of 3 and 6 nm, are found in all the drawn films, irrespective of draw-ratio; all, that is, except the very highest strength film. In this case the high angles give a width of 6 nm and the 'difference' gives 9 nm indicating very much more 'register' of fibrils. (In the perpendicular direction, similar measurements give a fibril size of ~4 nm with a 'difference' value of 8 nm.)

It should be possible to estimate the relative numbers of the two sizes of fibrils from the ratio of the intensity intercepts for the tangents to each curve in *Figure 9*. However, the experimental results are not precise enough to do this; indeed the results of *Figure 9*, which correspond to different diffraction spots for the same pattern, give different values for this ratio, possibly because the specimen was not precisely perpendicular to the incident X-ray beam.

The angle between the draw direction and the direction joining the centre of the 4-point low angle pattern and a maximum is consistently about 62° (for the 2-point pattern it is, of course, approximately 0°). Naively we may assume that the crystallites of the fibrils have surfaces whose normals are parallel to this direction. It is worthy of note, although we will not discuss it further here, that this is very close to the orientation of the low-index $(\bar{1}01)$ crystal plane of PET (~67°, 8°).

The interpretation of a curved log plot (*Figure 9*) is dependent entirely on the particular model employed, but according to several different models, the gradient at very low angles gives a loaded value for the 'coherence width' of the diffraction unit, which in the case of the data of *Figure 9* is between 3 and 6 nm, and should be similar to the size of crystal measured from wide-angle measurements. A comparison (*Figure 7*) shows good agreement of size, particularly if it is recalled that the wide-angle measurements will underestimate the size, the underestimate being most severe for the least-drawn film. Clearly the crystals responsible for wide-angle diffraction must be the same as the units responsible for low-angle diffraction.

The above discussion has followed Hosemann's treatment, but it should be borne in mind that when applying it to PET

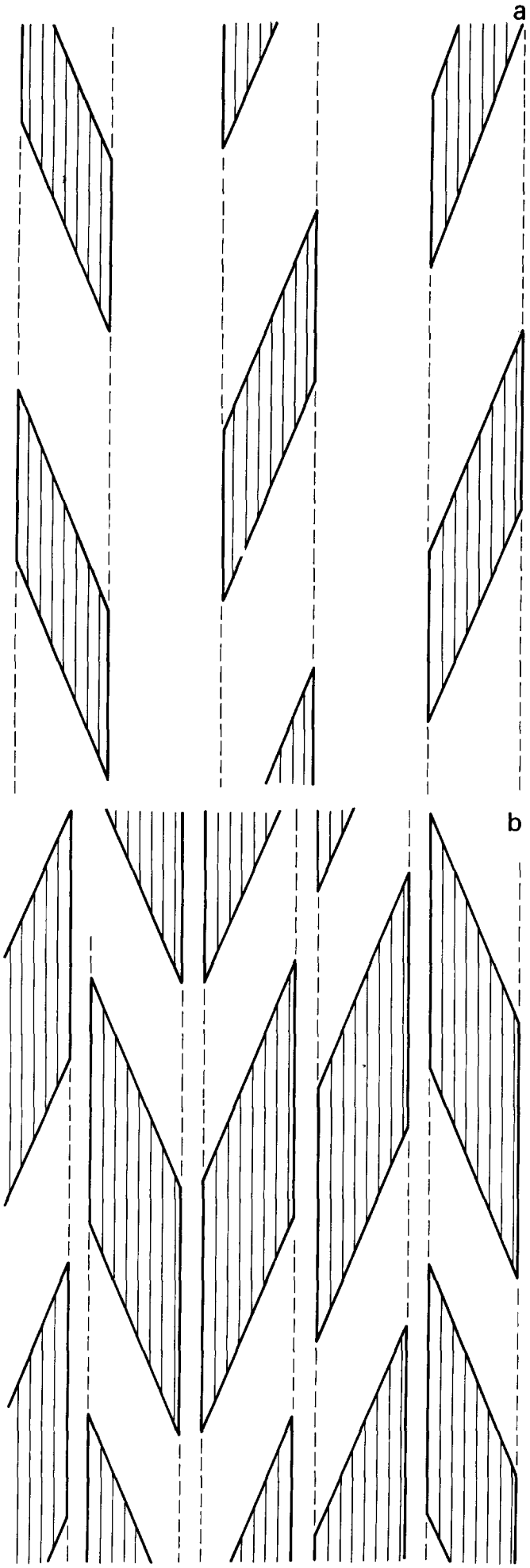

there are some inherent assumptions. Firstly it is difficult to imagine a paracrystal which would produce a four-point pattern unless one invokes a fibrillar model, and secondly, the patterns are very broad indeed. Hosemann's $\bar{f}^2$ is always taken to be a Gaussian form, but according to Guinier and Fournet[23], for wide patterns this is true only for rather special shapes of diffracting object. The deviation is not very big, however, even for the large scattering angles involved in this study. For example an isolated spherical particle of the same diameter as obtained here for the fibril width would give a Guinier plot whose gradient would be only 10% different in the large angles we measure, from that at the origin. Luckily the 'brick' of the present PET paracrystalline lattice turns out to be close to the optimum shape, and the consistent nature of the results appears to vindicate the assumptions.

For reasons just outlined, the numbers must be used cautiously, but it is possible to understand more about the fibril sizes by estimating the interfibrillar distances in the films. We assume that all the crystalline material is found in fibrils, and we use the measured density to calculate the volume fraction occupied by crystals. Knowing the average *c*-axis length of the crystals from wide-angle X-ray measurements and the long period from low-angle measurements (which remained constant at about 15 nm for all of the films), we can then estimate the proportional cross-sectional area occupied by fibrils. Thus we obtain an estimate of the distance between adjacent fibrils.

The density of the non-crystalline regions has been taken as being 1375 kg/m^3. This is not the same as the amorphous density and it might depend a little on draw-ratio, but it agrees with other measurements we have made and with some in the literature[24,25]. The choice of a value for the crystalline density is complicated by the recent proposal of a new unit cell[15], and by the likely variation of crystalline density in a real material, due to imperfections. This latter effect is discussed in detail by Fischer and Fakirov[21]. However, for this calculation we have taken it as 1455 kg/m^3 obtained from Daubeny and Bunn's unit cell. From this information and the assumption that each fibril is 3 nm x 4 nm in cross-section, the model of *Figure 10a* has been constructed for the film drawn 3.5:1, where the fibrils are well separated. (The regular spacing of the fibrils in *Figure 10a, Figure 10b* is for convenience of drawing only – the spacing is in practice expected to be rather irregular.) As the draw increases we find more fibrils per unit volume, so they are found closer together. The model predicts for the film drawn 6.5:1 (*Figure 10b*), still on the assumption of 3 nm fibrils, a distance of only 0.6 nm, or two molecular spacings, between fibrils; the model has clearly become unrealistic. Instead the fibrils join up. The predicted space between 6 nm fibrils for example is about 1.4 nm.

CONCLUSION

It is always a feature of low-angle X-ray scattering experiments that their interpretation cannot be unambiguous, and a model must be invoked. In the present work we have seen that the microfibrillar approach, using the methods of Hosemann, can give results which are consistent with wide-angle data. As well as the good agreement on the fibril

Figure 10 (a) Model of fibril structure of the lowest drawn film, viewed parallel to direction 2 in *Figure 2*. (b) The corresponding structure for the most highly drawn film

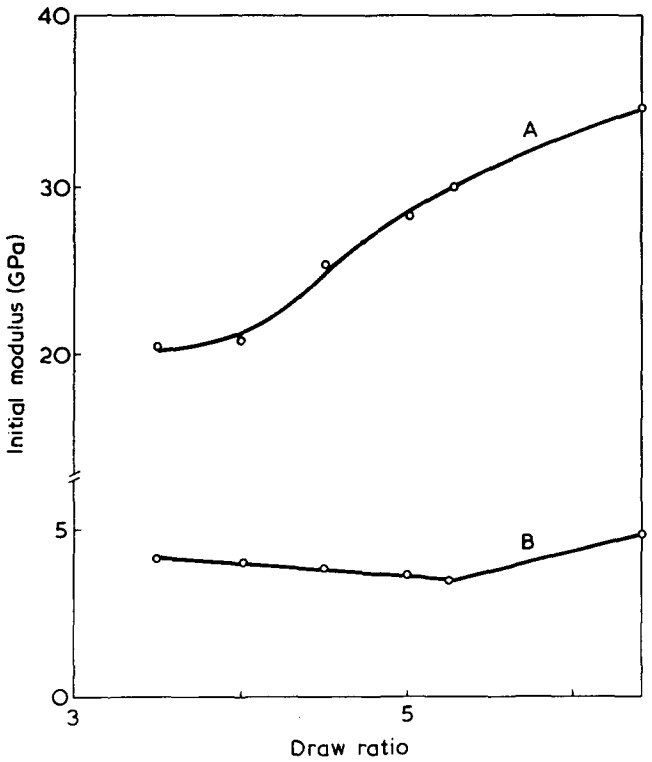

Figure 11 Zero-strain modulus as a function of draw ratio: A, draw direction; B, transverse direction

width (from low angle measurements) and crystallite width (wide angles), evidence from both techniques points to a 'limiting draw-ratio'. In the case of wide-angle diffraction the *c*-axis tilt approaches zero as the draw-ratio increases, and the maximum draw-ratio achievable without film snapping showed a trend towards 'space filling' by the microfibrils, a rather simple model indicating that in the highest drawn film the fibrils were frequently 'joining up' in a transverse direction because of their close packing. An interesting mechanical correlation with this structural behaviour is seen in measurements of the transverse direction modulus in *Figure 11*. As the films are further and further drawn the transverse modulus decreases slightly, as might be expected since molecules are becoming more oriented in the draw direction. This correlates with an increasing modulus in the draw direction. However, for the strongest film, even though the orientation in the draw direction is even greater, and the draw direction modulus higher, the transverse modulus has actually increased.

Clearly the modulus cannot be predicted by orientation measurements alone, and we must take the detailed morphology into account. Perhaps in this case, the 'joining-up' of fibrils described above produces a transverse crystalline link through the material, thus increasing modulus.

ACKNOWLEDGEMENTS

The author wishes to thank Dr D. J. Blundell for his invaluable help and encouragement during the course of this work, and Mr K. V. Gotham and Mr K. Beare for supplying the mechanical properties data.

REFERENCES

1 Hughes, M. A. and Sheldon, R. P. *J. Appl. Polym. Sci.* 1964, **8**, 1541
2 Dulmage, W. J. and Geddes, A. L. *J. Polym. Sci.* 1958, **31**, 499
3 Heffelfinger, C. J. and Burton, R. L. *J. Polym. Sci.* 1960, **47**, 289
4 Daubeny, R. de P., Bunn, C. W. and Brown, C. J. *Proc. Roy. Soc. (London) (A)* 1954, **226**, 531
5 Asano, T. and Seto, T. *Rep. Prog. Polym. Phys. Jpn* 1968, **11**, 175
6 Heffelfinger, C. J. and Schmidt, P. G. *J. Appl. Polym. Sci.* 1965, **9**, 2661
7 Statton, W. O. and Goddard, G. M. *J. Appl. Phys.* 1957, **28**, 1111
8 Bonart, R. *Kolloid Z. Z. Polym.* 1964, **199**, 136
9 Yeh, G. S. Y. and Geil, P. H. *J. Macromol. Sci. (B)* 1967, **1**, 251
10 Heffelfinger, C. J. and Lippert, E. L. *J. Appl. Polym. Sci.* 1971, **15**, 2699
11 Fischer, E. W., Goddar, H. and Schmidt, G. F. *Kolloid Z.Z. Polym.* 1968, **226**, 30
12 Holdsworth, P. J. ICI Plastics internal report
13 Dumbleton, J. H. and Bowles, B, B. *J. Polym. Sci. (A-2)* 1966, **4**, 951
14 Bhatt, G. M., Bell, J. P. and Knox, J. R. *J. Polym. Sci. (A-2)* 1976, **14**, 373
15 Fakirov, S., Fischer, E. W. and Schmidt, G. F. *Makromol. Chem.* 1975, **176**, 8, 2459
16 Yeh, G. S. Y., Hosemann, R., Loboda-Čačković, J. and Čacković, H. *Polymer* 1976, **17**, 309
17 Alexander, L. E. 'X-ray Diffraction methods in Polymer Science', Wiley, New York, 1969
18 Bonart, R. and Hosemann, R. *Kolloid Z.Z. Polym.* 1962, **186**, 16
19 Peterlin, A. *Colloid Polym. Sci.* 1975, **253**, 809
20 Takayanagi, M., Imada, K. and Kajiyama, T. *J. Polym. Sci. (C)* 1966, **15**, 263
21 Fischer, E. W. and Fakirov, S. *J. Mater. Sci.* 1976, **11**, 1041
22 Ferracini, E., Ferrero, A., Loboda-Čačkovic, J., Hosemann, R. and Čačković, H. *J. Macromol. Sci. (B)* 1974, **10**, 97
23 Guinier, A. and Fournet, G., 'Small angle scattering of X-rays', Wiley, New York, 1955
24 Farrow, G. *J. Appl. Polym. Sci.* 1960, **3**, 365
25 Nobbs, J. H., Bower, D. I. and Ward, I. M. *Polymer* 1976, **17**, 25